Tests of the accuracy of a data reduction method for determination of acoustic backscatter coefficients

Michael F. Insana,[a] Ernest L. Madsen, Timothy J. Hall, and James A. Zagzebski
Department of Medical Physics, University of Wisconsin, Madison, Wisconsin 53706

(Received 9 May 1985; accepted for publication 19 December 1985)

The accuracy of a new method for measuring ultrasonic backscatter coefficients was tested, using narrow-band pulses and well-defined media having scatterers randomly distributed in space. Experimentally determined values agree very well with theoretical values for wide ranges of experimental parameters, these ranges being applicable in measurements made on human soft tissues. An important outcome is that the method yields accurate results for scattering media positioned anywhere from the nearfield through the farfield of the nonfocused transducers employed. In addition, backscatter coefficients can be determined for a broad range of gate durations.

PACS numbers: 43.20.Fn, 43.20.Ye, 43.35.Yb

INTRODUCTION

A new method for reducing echo signal data to obtain accurate ultrasonic backscatter coefficients has been reported.[1] Other methods for measuring backscatter coefficients are carefully reviewed in that article: A detailed comparison of the present method with those other methods is also presented there. The new method is applied, in the present work, to the situation in which an ultrasound transducer transmits a pulsed sound beam and detects echo signals due to scattering in the medium. The volume of interest is selected by time-gating the received signal. The method employs accurately modeled pressure beam characteristics, completely accounts for pulser–receiver instrumentation, and—most importantly—is applied in terms of the actual frequency and time domains inherent in the data acquisition. The method is applicable for scattering volumes at any distance from the transducer surface, for broad ranges of pulse and gate duration, and for focused or nonfocused transducers. Contained in Ref. 1 is a detailed mathematical description of the method and preliminary results testing the accuracy for the case of narrow-band pulses. Using phantoms with well-defined ultrasonic properties, backscatter coefficients determined with the method for frequencies from 1–6 MHz agreed with those deduced independently based on the theory of Faran,[2] the latter requiring knowledge of the physical properties and geometry of the scatterers and knowledge of the number of scatterers per unit volume.

These preliminary results are very limited in terms of the experimental parameters employed. In particular, the pulse and gate durations were restricted to 10 and 25 μs, respectively, the distance between the transducer face and the "center" of the gated region was restricted to 20 cm, and only one size of glass bead scatterers was involved.

In the present work, more extensive tests of the method are reported. The accuracy of the method is again tested using phantoms with well-defined ultrasonic properties, and the results are compared with independent calculations.[2] In addition, the claim that the method is independent of transducer-to-scatterer-volumes distance and of gate duration is tested over a broad range of these parameters. Two different phantom materials were used, the size and concentration of the scatterers being different in each.

The expected accuracy of the data reduction method results from accounting for the physics of the measurement exactly except for one approximation regarding the source distribution on the transducer face and three approximations regarding the scattering medium.[1]

The transducer source distribution is assumed to consist of a set of equivalent point sources acting in unison and uniformly distributed over an area corresponding to the active element of the transducer. Comparison between this model and experiment shows excellent agreement for axial distances beyond 3 or 4 cm from the transducer face[3,4]; thus this approximation appears to be an excellent one.

The three approximations made regarding the scattering medium are as follows. First, the wave fronts of the scattered wave from each scatterer are assumed to be spherical in the region of the transducer face. This condition applies only if the scatterers are monopolar or if the scatterer is sufficiently distant from the transducer face. This approximation is applied to facilitate large-scale savings in computer time by allowing a double integral to be reduced to a single (numerical) integral. Second, it is assumed that the scatterers are randomly distributed in space and that the averge number per unit volume is small enough that the only (apparent) coherent scattering is related to the onset and termination of the time gate. Third, for calculational convenience the data reduction assumes that all scatterers are discrete and identical.

I. THE METHOD OF DATA REDUCTION

This section is a summary of the method of data reduction for determining the backscatter coefficient $\eta(\omega_0)$ at frequency ω_0.

[a] Present address: Center for Devices and Radiological Health, Rockville, MD 20857.

 0001-4966/86/051230-07$00.80

One of the principal relations involved is

$$\overline{||V_s(\omega)||^2} = \left(\frac{\tau}{2\pi}\right)^2 \left(\bar{N} \iiint_{\Lambda} d\mathbf{r} ||J(\omega,\mathbf{r},\tau)||^2 + \bar{N}^2 \left|\left| \iiint_{\Lambda} d\mathbf{r} J(\omega,\mathbf{r},\tau) \right|\right|^2 \right), \quad (1)$$

where ω is the angular frequency and $||V_s(\omega)||$ is the modulus of the Fourier transform of the echo signal $V_s(t)$. [The bar over the left side of Eq. (1) denotes taking the average of many realizations of $||V_s(\omega)||^2$.] τ is the gate duration; Λ is the volume of the scattering medium:

$$J(\omega,\mathbf{r},t) \equiv \int_{-\infty}^{\infty} d\omega'\, T(\omega') B_0(\omega') \Psi(\omega') \times \operatorname{sinc}\left(\frac{(\omega-\omega')\tau}{2\pi}\right) A_0^2(\mathbf{r},\omega') ; \quad (2)$$

$T(\omega')$ is the complex receiver transfer function; $B_0(\omega')$ is a complex superposition coefficient defining the pressure pulse in terms of the complete set of functions $A_0(\mathbf{r},\omega')$ corresponding to the transducer geometry[3,4]; and $\Psi(\omega')$ equals $\Phi_{\omega'}(\theta)$ at $\theta = 180°$, where $\Phi_{\omega'}(\theta)$ is the angle distribution factor described on p. 426 of Ref. 5 in terms of the asymptotic form of the scattered pressure wave amplitude $p_s(R,\theta)$. In particular, $\Phi_{\omega'}(\theta) = (R/A)e^{-ik'R}p_s(R,\theta)$, where R is the (large) distance from the scatterer to the field point, A is the amplitude of the incident plane wave, ω' is the angular frequency, and $k' = k(\omega')$ is the complex wavenumber.

Also, $\operatorname{sinc} x \equiv \sin(\pi x)/(\pi x)$. The sinc function in Eq. (2) is the Fourier transform of the rectangular gating function

$$g(t) = \begin{cases} 1, & -\tau/2 \leqslant t \leqslant \tau/2 , \\ 0, & \text{otherwise} , \end{cases}$$

evaluated at angular frequency $\omega - \omega'$. Notice that $J(\omega,\mathbf{r},\tau)$ is a convolution in frequency of the sinc function with the remainder of the integrand. The importance of accounting for this convolution in determining accurate backscatter coefficients was pointed out previously.[6]

Equation (1) states that the square of the measured echo signal spectrum is composed of two parts [neglecting the common factor $(\tau/2\pi)^2$]:

$$\bar{N}a(\omega) = \bar{N} \iiint_{\Lambda} d\mathbf{r} ||J(\omega,\mathbf{r},\tau)||^2 \quad (3a)$$

and

$$\bar{N}^2 b(\omega) = \bar{N}^2 \left|\left| \iiint_{\Lambda} d\mathbf{r} J(\omega,\mathbf{r},\tau) \right|\right|^2 . \quad (3b)$$

The first part, $\bar{N}a(\omega)$, is proportional to the average number of scatterers per unit volume ($\bar{N}$) and is the result of incoherent scattering from the random distribution of point scatterers throughout Λ. The second part, $\bar{N}^2 b(\omega)$, is proportional to the square of the average concentration of scatterers. It describes the coherent scattering contribution to $v_s(t)$ due to the onset and termination of the time gate. (See the Appendix of Ref. 1 for a discussion of why coherent scattering is expected to occur at the onset and termination of the time gate.) Notice that although $a(\omega)$ and $b(\omega)$ look similar, they are quite different in that the phase of J is included in the volume integration for $b(\omega)$, whereas only the modulus of the complex function $J(\omega,\mathbf{r},\tau)$ is involved in $a(\omega)$.

When sufficiently long gate durations and pulse durations are used to acquire backscatter waveform data, $J(\omega,\mathbf{r},\tau)$ will peak strongly at ω_0, the center frequency of the pulse. Two new functions can then be defined from Eq. (2) and Eqs. (3a) and (3b):

$$\bar{N}a(\omega_0) \equiv \bar{N} ||\Psi(\omega_0)||^2 a'(\omega_0) \quad (3c)$$

and

$$\bar{N}^2 b(\omega_0) \equiv \bar{N}^2 ||\Psi(\omega_0)||^2 b'(\omega_0) . \quad (3d)$$

Thus we restrict ourselves in the following discussion to gated echoes following the transmission to narrow-band pulses. The backscatter coefficient $\eta(\omega_0)$ is defined as the differential scattering cross section per unit volume at a scattering angle of 180°. For a single scatterer having spherical symmetry, the differential scattering cross section for scattering angle θ, $d\sigma_{\omega_0}(\theta)/d\Omega$, is defined to be the power scattered per unit solid angle (far from the scatterer) divided by the incident plane-wave intensity. If A is the incident pressure wave amplitude, the incident intensity is $||A||^2/(2\rho c)$. Also, the power scattered per unit solid angle is

$$\frac{||p_s(R,\theta)||^2}{2\rho c} \frac{R^2 d\Omega}{d\Omega} = \frac{R^2 ||p_s(R,\theta)||^2}{2\rho c} .$$

Therefore,

$$\frac{d\sigma_{\omega_0}(\theta)}{d\Omega} = \frac{R^2 ||p_s(R,\theta)||^2}{||A||^2} = ||\Phi_{\omega_0}(\theta)||^2 ,$$

where $\Phi_{\omega_0}(\theta)$ was defined above. Also, for $\theta = 180°$, we introduced the following definition above: $\Psi(\omega_0) \equiv \Phi_{\omega_0}(\theta)$. Thus $d\sigma_{\omega_0}(\theta)/d\Omega = ||\Psi(\omega_0)||^2$. The backscatter coefficient for spatially random distributed scatterers then becomes

$$\eta(\omega_0) \equiv \bar{N} ||\Psi(\omega_0)||^2 = \frac{\overline{||V_s(\omega_0)||^2}}{(\tau/2\pi)[a'(\omega_0) + \bar{N}b'(\omega_0)]} , \quad (4)$$

where $\bar{N}$ is the mean number of scatterers per unit volume. Computation of the quantities of $a'(\omega_0)$ and $b'(\omega_0)$ requires determination of the product $T(\omega)B_0(\omega)$ over a sufficiently large band of frequencies about ω_0. This requires recording the echo from a reference reflector.

Many practical situations exist in which $\bar{N}$ is not easily defined (e.g., soft tissues) or not known at the time of measurement (e.g., studies in tissue phantoms). It has been shown,[1] however, that for sufficiently long gate durations τ,

$$\bar{N}b'(\omega_0)/a'(\omega_0) \underset{\substack{\tau \text{ large} \\ \text{enough}}}{\longrightarrow} 0 . \quad (5)$$

For measurement conditions in which Eq. (5) holds, Eq. (4) can be reduced to

$$\eta(\omega_0) \simeq \overline{||V_s(\omega_0)||^2}/[(\tau/2\pi)^2 a'(\omega_0)] . \quad (6)$$

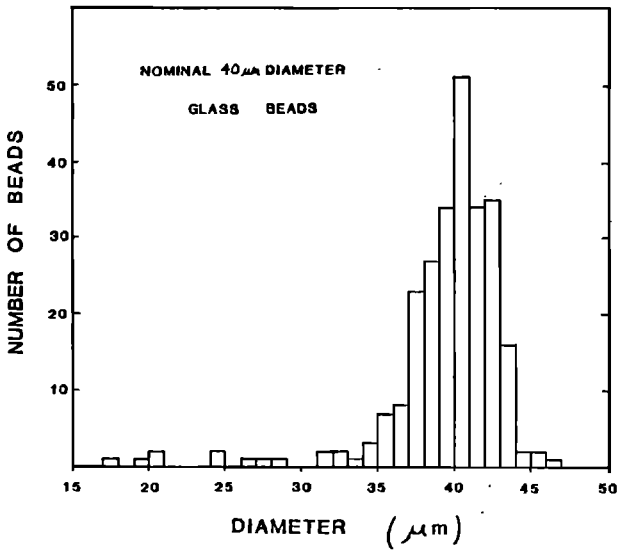

FIG. 1. Histogram of the diameter distribution of the glass bead scatterers in sample 1. Measurements were done using an optical microscope with a calibrated ocular micrometer.

It is convenient to define the quantity

$$\zeta(\omega_0) \equiv \overline{||V_s(\omega_0)||^2}/[(\tau/2\pi)^2 a'(\omega_0)]\,,$$

applying for *any* τ, and to write Eq. (6) in the form

$$\zeta(\omega_0) \underset{\substack{\tau \text{ sufficiently} \\ \text{large}}}{\rightarrow} \eta(\omega_0)\,.$$

One of the objectives in the work reported is to determine combinations of pulse duration and gate duration (τ) for which $\zeta(\omega_0) \approx \eta(\omega_0)$.

II. MATERIALS

Two samples consisting of glass bead scatterers randomly distributed in agar were used to test the accuracy of the data reduction analysis. In sample 1, the glass spheres exhibit a strong peak in their diameter distribution at 40 μ. The mean concentration of scatterers is $\overline{N} = 46$ scatterers per mm^3. The scatterers in sample 2 are spheres of the same type of glass, also having narrow diameter distribution with a 59-μ mean diameter. The mean scatterer concentration for sample 2 is $\overline{N} = 7.7$ scatterers per mm^3. Measurements of the diameter distributions were done using an optical microscope with a calibrated ocular micrometer. Histograms for the diameter distributions are shown in Fig. 1 (sample 1) and Fig. 2 (sample 2). Mean concentrations of scatterers were found by counting the number of beads in a thin slab of the material, the mass of the slab and its density also having been determined.

Measurements of speed of sound and attenuation coefficients were made using a through-transmission technique[7] at 20 °C at five discrete frequencies between 1 and 7 MHz. Curve fitting was done assuming that the attenuation coefficient $\alpha(f)$ is proportional to a power of the frequency f: $\alpha(f) = \alpha_0 f^n$, where α_0 and n are constants and f is the frequency. For sample 1, $\alpha_0 = 0.052$ dB cm^{-1} MHz$^{-1.5}$ and $n = 1.5$. For sample 2, $\alpha_0 = 0.055$ dB cm^{-1} MHz$^{-1.4}$ and $n = 1.4$.

Backscatter coefficients for these samples were computed independently using the theory of Faran.[2] Required parameters for the glass beads were the density (2.4 g/cm^3), Poisson's ratio (0.21), and the longitudinal speed of sound (5570 m/s). The agar was taken to be waterlike with the density of 1.00 g/cm^3 and a speed of sound of 1525 m/s (our measured values). Faran's theory accounts for both longitudinal and transverse waves and has been found to agree with experiment for direct measurements of differential scattering cross sections over a broad range of scattering angles and frequencies.[8] Assuming incoherent scattering only, the calculated, or "theoretical," backscatter coefficient (defined as the differential scattering cross section per unit volume for a 180° scattering angle) is given by $\eta_{\text{theory}}(\omega_0) = \overline{N} d\sigma/d\Omega|180°$. Because the backscattered intensity for small scatterers is a strong function of scatterer diameter, $\eta_{\text{theory}}(\omega_0)$ for each sample was calculated as a weighted average using the histograms in Figs. 1 and 2; i.e.,

$$\eta_{\text{theory}}(\omega_0) = \sum_{i=1}^{L} f_i \eta_i(\omega_0)\,,$$

where f_i is the number fraction of scatterers (particles) in the ith bin and $n_i(\omega_0)$ is the calculated backscatter coefficient corresponding to the diameter of the scatterers in the ith bin.

III. EXPERIMENTAL PROCEDURE

A block diagram of the equipment used to obtain scattered echo signals from the sample is shown in Fig. 3. The sample was placed in water at a specific distance from the transducer. Nonfocused 13-mm-diam transducers were used to transmit narrow-band pulses and receive the backscattered echoes. The pulse repetition frequency was adjusted such that echoes from the entire sample were received before the next pulse was transmitted. From these echo signal waveforms, axial regions of interest were selected via time gate positioning. Using the Biomation 8100 transient recorder, 25 time-gated echo signal waveforms were then recorded, each corresponding to a different position of the transducer beam axis through the sample. These different

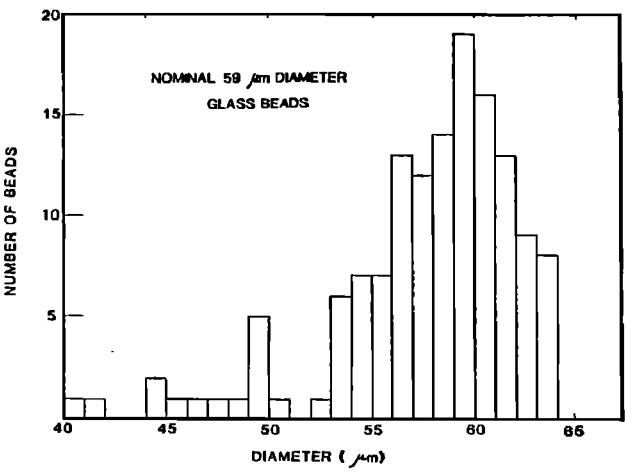

FIG. 2. Histogram of the diameter distribution of the glass bead scatterers in sample 2. Measurements were done using an optical microscope with a calibrated ocular micrometer.

positionings were accomplished by translating the sample perpendicularly to the beam axis in a raster fashion. The Fourier transforms of each of these 25 waveforms were then computed yielding values of $V_s(\omega_0)$ contained in the numerator of Eq. (4). The mean value of the square of the moduli of these Fourier transforms then yields the numerator of Eq. (4), viz., $\overline{||V_s(\omega_0)||^2}$.

To account for pulser–receiver characteristics for each set of experimental parameters, a recording was made of the echo signal waveform due to reflection from a planar Lucite[9]-to-water interface placed at half the transducer-to-sample distance. This reflector position was chosen so that the echo pressure wave received most closely represents that incident on the involved scatterers.[10] This echo waveform allows the determination of the (complex) function $B_0(\omega)T(\omega)$. Care was taken to maintain the same transmission and reception conditions for recording the plane reflector signal as those for recording the scatter signals from the sample.

All data acquisition and storage in these measurements were under control via an LSI 11/23 microcomputer.[11] The data sampling rate of the transient recorder was 20 MHz. Further details regarding experimental techniques can be found in Ref. 12.

IV. NUMERICAL METHODS

All data reduction was done on a PDP 11/23-PLUS* computer configured with an array processor.[13] Discrete Fourier transforms of echo signal waveforms were computed according to Bracewell.[14]

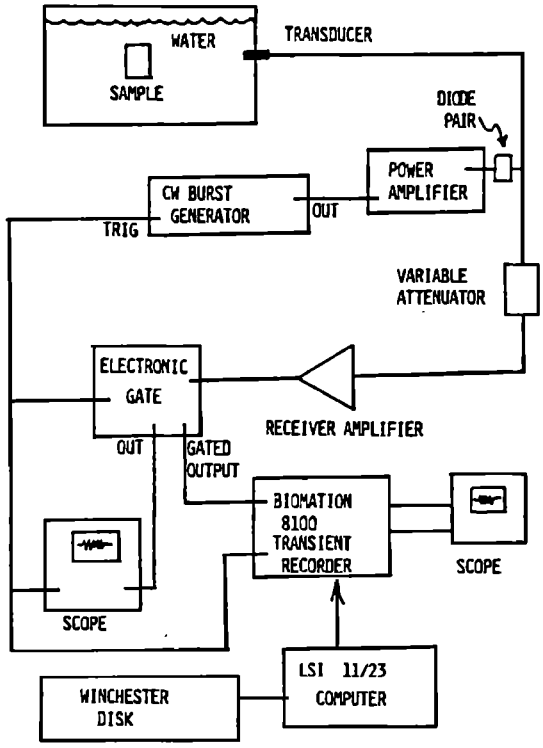

FIG. 3. Block diagram of the experimental apparatus for acquiring and storing data.

The quantity

$$\zeta(\omega_0) \equiv \left[\overline{||V_s(\omega_0)||^2}/(\tau/2\pi)^2 a'(\omega_0) \right]$$

was determined for each measurement; thus values of $b'(\omega_0)$ shown in Eq. (4) were never needed. Recall that $\zeta(\omega_0) \to \eta(\omega_0)$ for sufficiently large gate duration τ.

Numerical integrations over volume and frequency were done to determine values of $a'(\omega_0)$ which has the form

$$a'(\omega_0) = \iiint_{\Lambda} d\mathbf{r} \left| \left| \int_{\infty}^{-\infty} d\omega' T(\omega') B_0(\omega') \times \operatorname{sinc}\left(\frac{(\omega_0 - \omega')\tau}{2\pi} \right) A_0^2(\mathbf{r},\omega') \right| \right|^2 . \quad (7)$$

The trapezoidal rule was used throughout. Computing time was minimized without compromising accuracy by judicious choice of integration limits and intervals. It was found that the frequency integral converges when the lower limit of integration is less than $\omega_0 - 6\pi/\tau$ and the upper limit is greater than $\omega_0 + 6\pi/\tau$, where τ is the gate duration (time). This range of frequencies includes the five mainlobes of the sinc function. Thirty-one frequency values were necessary for convergence of the frequency integral. Considerable savings in computer time resulted from introducing a Taylor series expansion of the expression for $A_0(\mathbf{r},\omega)$ about ω_0.

The pressure field has axial symmetry so that the volume integral in Eq. (7) was reduced to two dimensions: radial and axial. The volume integration limits extend over the entire sample volume Λ. However, a smaller integration volume, Λ' having lateral margins extending through the first sidelobe of the pressure field and containing at least 80 points over that radial distance, was used with no loss of accuracy. Axially, Λ' must have a length of at least $L = c_s(\tau/T)/2$, where c_s is the speed of sound in the scattering medium and T is the pulse duration. The distance d between the transducer face and the proximal end of Λ' must be no greater than

$$d = d_w + (c_s/2)(t_{on} - T - 2d_w/c_w) ,$$

where d_w is the water path distance from the transducer to the sample, c_w is the speed of sound in water, and t_{on} is the onset time of the electronic gate relative to a zero time corresponding to the beginning of the emission of the pulse from the transducer. The distance between the distal end of Λ' and the transducer face must be no less than $d + L$. In fact, Λ' should be extended over a somewhat larger axial extent than that defined here to account for the fact that the boundaries separating scatterers contributing from those not contributing are not simply planes perpendicular to the axis of symmetry of the beam.[1,6] An axial integration increment of less than $2\lambda_0$ (where $\lambda_0 = 2\pi c_s/\omega_0$) was found to be sufficient to maintain accuracy.

V. RESULTS

In Fig. 4 are plotted values of

$$\zeta(\omega_0) \equiv \left[\overline{||V_s(\omega)||^2}/(\tau/2\pi)^2 a'(\omega_0) \right]$$

for various gate durations τ between 4 and 20 μs, all other parameters being fixed. Sample 1, containing 40-μ-diam beads, was used in this study; the center frequency ω_0 was 2.00 MHz, and the pulse duration was 5 μs. The transducer-to-scattering-volume distance was maintained at 10 cm. The horizontal dashed line corresponds to the theoretical value.

In Fig. 5 are shown values of $\zeta(\omega_0)$ where τ is again the only variable, the latter varying between 6 and 30 μs. All other parameters are the same as those corresponding to Fig. 4 except that the frequency in this case was 5.00 MHz.

In Figs. 6 and 7 are shown determinations of backscatter coefficients for cases in which the varying parameter is the distance of the scattering region from the transducer. Sample 2 was used in this study. The frequency was 2.00 MHz in Fig. 6 and 4.00 MHz in Fig. 7. Again, parameters other than the distance from the transducer were held fixed in both cases, the pulse duration having been 5 μs and the gate duration, 10 μs.

In Tables I and II are shown comparisons of measured backscatter coefficients and the Faran values for eight frequencies between 1 and 6 MHz. Table I corresponds to sample 1 (40-μ-diam beads) and Table II corresponds to sample 2 (59-μ-diam beads). All measurements involved pulse durations of at least 5 μs and gate durations of at least 10 μs.

All error specifications, shown in the form of error bars in Figs. 4–7 and numerically in Tables I and II, correspond to the standard deviations of the means.[15]

VI. DISCUSSION

As argued in Ref. 1 and summarized in Sec. I of this report, the coherent term in the denominator of Eq. (4) $[\bar{N}b'(\omega_0)]$ becomes negligible for large enough gate duration, τ: i.e.,

$$\zeta(\omega_0) \equiv \frac{\overline{||V_s(\omega_0)||^2}}{(\tau/2\pi)^2 a'(\omega_0)} \underset{\text{large } \tau}{\overset{\text{sufficiently}}{\longrightarrow}} \eta(\omega_0) .$$

One of the major objectives in the work reported is to gain an insight into the dependence of $\zeta(\omega_0)$ on the gate duration and frequency for some reasonable pulse duration. The results of the gate duration studies shown in Figs. 4 and 5 (2 and 5 MHz, respectively) indicate that, for 5-μs pulse durations and the ranges of gate durations employed, there is negligible dependence of $\zeta(\omega_0)$ on gate durations. Thus a pulse duration of 5 μs and gate duration of 6 μs or higher are adequate to ensure that $\zeta(\omega_0)$ is a good approximation to the backscatter coefficient $\eta(\omega_0)$. This criterion was used in setting $\zeta(\omega_0)$ equal to $\eta(\omega_0)$ in the results displayed in Figs. 6

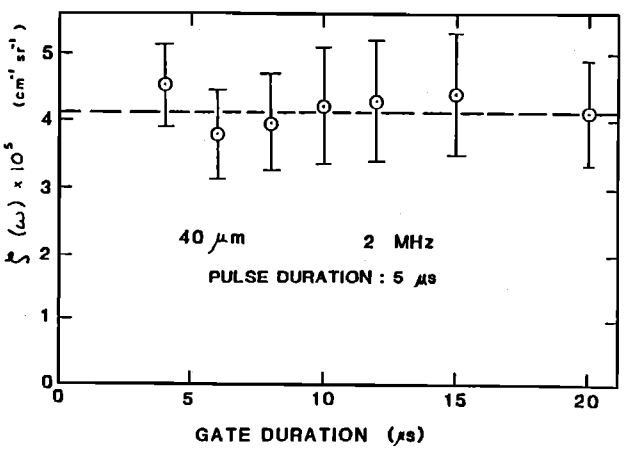

FIG. 4. Plotted values of $\zeta(\omega_0) \equiv [\overline{||V_s(\omega_0)||^2}/(\tau/2\pi)^2 a'(\omega_0)]$, determined with the data reduction method on sample 1 at $\omega_0 = 2$ MHz and at various gate durations. The pulse duration was maintained at 5 μs. The horizontal dashed line corresponds to the theoretical value (via Faran, Ref. 2). The transducer-to-scattering-volume distance was 20 cm.

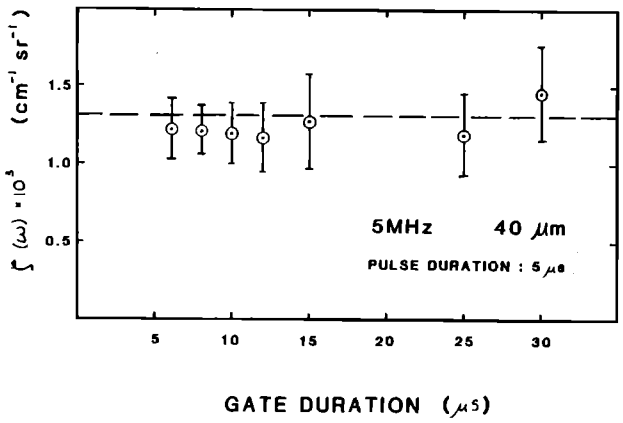

FIG. 5. Plotter values of $\zeta(\omega_0) \equiv [\overline{||V_s(\omega_0)||^2}/(\tau/2\pi)^2 a'(\omega_0)]$, determined with the method of data reduction on sample 1 at $\omega_0 = 5$ MHz and at various gate durations. The pulse duration was maintained at 5 μs. The horizontal dashed line corresponds to the theoretical value (via Faran, Ref. 2). The transducer-to-scattering-volume distance was 20 cm.

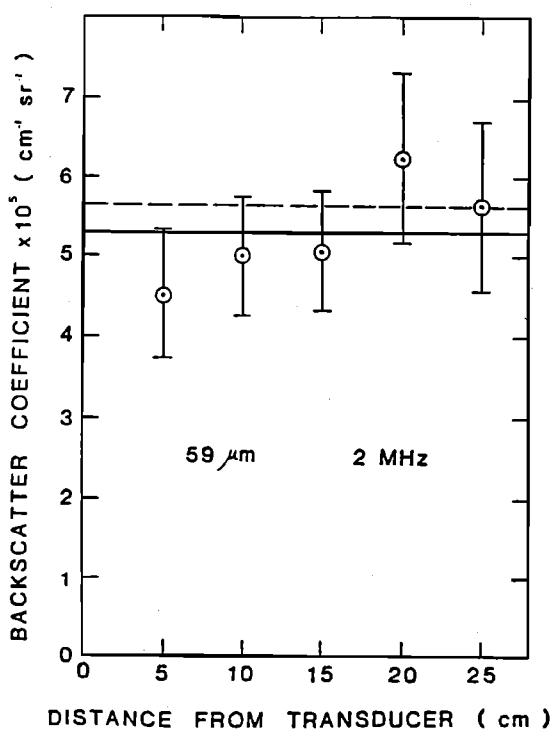

FIG. 6. Backscatter coefficients for sample 2 at 2 MHz for various distances between the transducer face and scattering volume interrogated. The pulse and gate durations were maintained at 5 and 10 μs, respectively. The horizontal solid line corresponds to the mean value of these experimental determinations and the horizontal dashed line corresponds to the theoretical value based on Faran (Ref. 2).

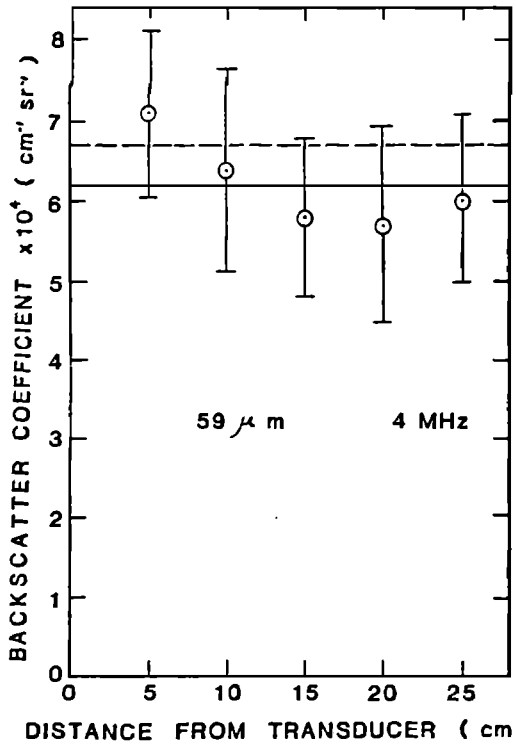

FIG. 7. Backscatter coefficients for sample 2 at 4 MHz for various distances between the transducer face and scattering volume interrogated. The pulse and gate durations were maintained at 5 and 10 μs, respectively. The horizontal solid line corresponds to the mean value of these experimental determinations and the horizintal dashed line corresponds to the theoretical value based on Faran (Ref. 2).

and 7 and Tables I and II. It is very important to note that the ratio of the coherent term to the incoherent is proportional to $\bar{N}$. Thus the result that $\zeta(\omega_0)$ is not approximately equal to $\eta(\omega_0)$ will be more likely observed for larger $\bar{N}$. A study employing considerably larger values of $\bar{N}$ than used in the present study is under way.

In Tables I and II, good agreement between theory and the results of our data reduction method is shown to exist for both samples over the frequency range from 1 to 6 MHz.

Perhaps the most important result of the present work has been the demonstration that backscatter coefficients determined using our method of data reduction are nearly independent of transducer-to-scattering-volume distance. The results at 2 MHz for five distances from 5–25 cm agree with one another and with the theoretical value. The mean experimental value, shown as the solid horizontal line, is about 6% below the theoretical value, shown as the dashed horizontal line. In Fig. 7, the results for 4 MHz also show reasonably good agreement over the same range of transducer-to-scattering-volume distances, their mean value (solid horizontal line) being about 13% below the theoretical value (dashed horizontal line).

TABLE I. Theoretical and experimental backscatter coefficients at eight frequencies for test sample 1 in which the nominal scatterer diameter is 40 μ. The theoretical values were computed using the theory by Faran (Ref. 2).

Frequency (MHz)	Backscatter coefficient ($sr^{-1}\,cm^{-1}$)	
	Theory	Experiment
1.0	2.64×10^{-6}	$(3.35\pm0.64)\times10^{-6}$
1.2	5.45×10^{-6}	$(5.85\pm1.15)\times10^{-6}$
2.0	4.10×10^{-5}	$(4.45\pm0.88)\times10^{-5}$
2.5	9.79×10^{-5}	$(9.98\pm1.93)\times10^{-5}$
3.0	1.98×10^{-4}	$(1.50\pm0.26)\times10^{-4}$
4.0	5.84×10^{-4}	$(5.48\pm1.02)\times10^{-4}$
5.0	1.31×10^{-3}	$(1.09\pm0.22)\times10^{-3}$
6.0	2.44×10^{-3}	$(1.80\pm0.36)\times10^{-3}$

TABLE II. Theoretical and experimental backscatter coefficients at eight frequencies for test sample 2 in which the nominal scatterer diameter is 59 μ. The theoretical values were computed using the theory by Faran (Ref. 2).

Frequency (MHz)	Backscatter coefficient ($sr^{-1}\,cm^{-1}$)	
	Theory	Experiment
1.0	3.74×10^{-6}	$(3.32\pm0.54)\times10^{-6}$
1.2	7.69×10^{-6}	$(7.84\pm1.40)\times10^{-6}$
2.0	5.63×10^{-5}	$(5.31\pm1.21)\times10^{-5}$
2.5	1.32×10^{-4}	$(1.30\pm0.25)\times10^{-4}$
3.0	2.58×10^{-4}	$(2.92\pm0.58)\times10^{-4}$
4.0	7.08×10^{-4}	$(6.20\pm1.12)\times10^{-4}$
5.0	1.44×10^{-3}	$(1.45\pm0.24)\times10^{-3}$
6.0	2.37×10^{-3}	$(2.03\pm0.33)\times10^{-3}$

The general accuracy for the method of data reduction investigated also creates promise for the development of quantitative operator and instrument independent ultrasound grey scale imaging. In our data acquisition, an electronic time gate was employed. It is quite reasonable, however, to record the entire echo waveform corresponding to transducer-to-scattering-volume distances of, say, 5 through 25 cm. A time gate can then be applied computationally, selecting out any desired transducer-to-scattering-volume distance in that range. The possibility then presents itself to gather a sufficient number of independent waveforms in order to compute a mapping of backscatter coefficients as a function of position in the interrogated medium. This procedure will require concomittant determinations of attenuation coefficients; such determinations can be included in the data reduction as will be shown in subsequent reports. If the capacity to generate accurate quantitative grey scale images eventually can be achieved, this will represent a considerable advance of ultrasound imaging particularly in that such images would be operator and instrument independent.

Finally, some discussion of the accuracy of the calculated theoretical values for backscatter coefficients is appropriate. Values for the density, compressibility, and Poisson's ratio for the glass beads are parameters in the calculations. The accuracy of these three quantities provided by the manufacturer is difficult to ascertain, particularly since microscopic bubbles were observed in about 30% of the spheres. These bubbles are presumably gaseous as indicated by the apparent large difference in (optical) index of refraction between the material composing the bubbles and the glass. Even if the density, compressibility, and Poisson's ratio employed in the Faran calculations are correct mean values, the applicability of the Faran theory may be somewhat compro-

mised since it presumes two homogeneous materials only, that of which the spheres are composed and that of which the surrounding medium is composed. However, in view of the extensive good agreement between theoretical values and our mean experimental results, we believe that both our values and the Faran values are accurate to within 10% or 15%.

VII. CONCLUSIONS

Backscatter coefficients were measured for a well-defined scattering medium using a new method of data reduction described in Ref. 1. The results of measurements using narrow-band pulses agree very well with theory for a wide range of time gate durations and transducer-to-sample-volume distances, demonstrating the accuracy and flexibility of this technique.

For pulse durations of at least 5 μs and gate durations of at least 6 μs, we have found that the quantity

$$\zeta(\omega_0) \equiv \overline{||V_s(\omega_0)||^2}/[(\tau/2\pi)^2 a'(\omega_0)] ,$$

introduced at the end of Sec. II, is a good approximation of the backscatter coefficient $\eta(\omega_0)$, where ω_0 is the center frequency in radians per unit time. Thus coherent effects related to the onset and termination of the rectangular time gate for these pulse and gate durations are negligible in determining the backscatter coefficient.

On the basis of the results presented in Tables I and II and in Figs. 6 and 7, we also come to the most important conclusion that the determination of backscatter coefficients using the method of data reduction employed is accurate over broad ranges of frequencies (1–6 MHz) and transducer-to-scattering-volume distances (5–25 cm). This result also opens up the possibility for development of quantitative, operator, and instrument-independent grey scale imaging.

Finally, we remind the reader that only narrow-band pulses were involved in the study and that only nonfocused transducers were employed. Investigations using broad-band pulses and/or focused transducers are the subjects of future reports.

ACKNOWLEDGMENTS

This work was supported in part by NIH Grants R01-CA39224 and R01-CA25634. We also thank Colleen Schutz for her efficient generation of the typescript.

[1]E. L. Madsen, M. F. Insana, and J. A. Zagzebski, "Method of data reduction for accurate determination of acoustic backscatter coefficients," J. Acoust. Soc. Am. 76, 913–923 (1984).
[2]J. J. Faran, Jr., "Sound scattering by solid cylinders and spheres," J. Acoust. Soc. Am. 23, 405–418 (1951).
[3]E. L. Madsen, M. M. Goodsitt, and J. A. Zagzebski, "Continuous waves generated by focused radiators," J. Acoust. Soc. Am. 70, 1508–1517 (1981).
[4]M. Goodsitt, E. L. Madsen, and J. A. Zagzebski, "Field patterns of pulsed focused ultrasonic radiators in attenuating and nonattenuating media," J. Acoust. Soc. Am. 71, 318–329 (1982).
[5]P. M. Morse and K. U. Ingard, *Theoretical Acoustics* (McGraw-Hill, New York, 1968), Chap. 8, p. 426.
[6]R. C. Chivers and C. R. Hill, "A spectral approach to ultrasonic scattering from human tissues: Methods, objectives, and backscattering measurements," Phys. Med. Biol. 20, 799–815 (1975) (see, particularly, pp. 808–810).
[7]E. L. Madsen, J. A. Zagzebski, R. A. Banjavic, and R. E. Jutila, "Tissue-mimicking materials for ultrasound phantoms," Med. Phys. 5, 391–394 (1978).
[8]T. M. Burke, M. M. Goodsitt, E. L. Madsen, and J. A. Zagzebski, "Angular distribution of scattered ultrasound from a single steel sphere in agar gel: A comparison between theory and experiment," Ultrason. Imag. 6, 342–347 (1984).
[9]Lucite is a trade name for plymethyl methacrylate.
[10]In theory, the specific choice of the distance between the transducer and the plane reflector is not important; this flexibility depends on the accuracy of the beam model, however, and remains to be tested.
[11]Trademark of the Digital Equipment Corporation, Maynard, MA.
[12]M. F. Insana, Ph.D. thesis, University of Wisconsin, Madison, WI (1983).
[13]SKYMNK-Q, Sky Computers, Inc., Lowell, MA.
[14]R. N. Bracewell, *The Fourier Transform and Its Applications* (McGraw-Hill, New York, 1978).
[15]I. A. Sokolnikoff and R. M. Redheffer, *Mathematics of Physics and Modern Engineering* (McGraw-Hill, New York, 1966), 2nd ed., p. 643.